THE INVESTIGATION ON SYNTHESIS AND OPTICAL PROPERTIES OF Ag-DOPED ZnS NANOCRYSTALS BY HYDROTHERMAL METHOD

DEZHI QIN[*], GUANGRUI YANG[a], GUOXU HE, LI ZHANG, QIUXIA ZHANG, LUYAO LI

College of Chemistry and Chemical Engineering, Pingdingshan University, Pingdingshan 467000, P. R. China
[a]*Institute of Environmental and Municipal Engineering, North China University of Water Conservancy and Electric Power, Zhengzhou 450011, P. R. China*

Ag-doped ZnS nanocrystals were synthesized by hydrothermal method in propanetriol solutions. X-ray diffraction (XRD), energy dispersive X-ray spectroscopy (EDX), transmission electron microscopy (TEM) and high-resolution transmission electron microscopy (HRTEM) characterizations were used to determine the structure and morphology of ZnS: Ag nanocrystals. The as-prepared nanoparticles are approximately spherical with average size around 20~30nm and have a cubic zinc blended structure. The quantum-confined effect of the Ag-doped ZnS nanocrystals is confirmed by the ultraviolet-visible (UV-vis) spectra. The optical properties of ZnS: Ag nanocrystals were investigated by using photoluminescence (PL) spectra, which showed that the products exhibited good optical properties with maximum emission peak at about 460nm, and the intensity of luminescence increased with the increase of concentration of Ag ions.

1. Introduction

Over the last decades, nanometer-sized doped semi-conductors have received much attention due to their novel optical and electrical properties arising from their unique quantum-confined nature [1-4]. ZnS is an important type of II-VI semiconductor with direct and wide band gap of 3.66ev and widely used in flat-panel displays, photovoltaic devices, solar cells, field emission devices (FED), which is an attractive host for the formation of doped nanocrystals [5-8]. Comparing with undoped ZnS nanocrystals, the doping ions act as recombination centres for the excited electron-hole pairs and result in different optical properties [9]. Among these doped ZnS nanocrystals, ZnS: Mn, ZnS: Cu and ZnS: Ni have attracted considerable attention because of their relatively easy synthesis, unique properties and application in photoluminescence (PL) and electroluminescence (EL) fields [1-4, 10-13]. There have been very few studies on Ag-doped ZnS nanocrystals because the solubility of Ag_2S is much smaller than that of ZnS [$K_{sp}(Ag_2S) \ll K_{sp}(ZnS)$], which makes it difficult for Ag^+ and Zn^{2+} ions to co-precipitation [2, 14-16].

Many methods have been developed for the synthesis of doped ZnS nanocrystals, such as organometallic precursor method [17], sol-gel method [18], chemical co-precipitation [3],

---

[*]Corresponding author: dezhiqin@163.com

micro-assisted method [16] and chemical vapor deposition [13] *etc*. However, these techniques need high reaction temperature, toxic organic solvents or high cost of equipment and usually suffer some problems including poor crystallinity, particle agglomeration which significantly hinder their potential applications. Compared with conventional methods, hydrothermal synthesis has the advantage of rapid formation the crystal nuclei, narrow size distribution, and the reaction system is closed, which can effectively avoid oxidation phenomena and environmental pollution [2, 14, 19].

In this paper, we adopt hydrothermal method to synthesis Ag-doped ZnS nanocrystals by using propanetriol as capping agent. The optical properties of product were characterized by UV-vis adsorption and photoluminescence (PL) spectra. X-ray diffraction (XRD) and transmission electron microscopy (TEM) have also been carried out to study the structure and morphology of the Ag-doped ZnS nanocrystals.

2. Experimental

2.1 Synthesis of Ag-doped ZnS nanocrystals

Analytical grade $Zn(NO_3)_2•6H_2O$, $AgNO_3$, thioacetamide (TAA) and propanetriol were purchased from Sinopharm Chemical Regent Co., Ltd., P. R. China. Water used in all synthesis procedures was high purity grade with a conductivity of 18.2 $M\Omega•cm^{-1}$.

ZnS: Ag nanocrystals with different Ag ions concentrations were synthesis in water with propanetriol as capping agent. In a typical experiment, 0.02mol zinc nitrate, calculated amount of silver nitrate, 0.02mol TAA were dissolved in 50mL of 2% propanetriol solution. The pH of the mixed solution was adjusted to 9.6 with 4mol•L^{-1} NaOH solution and N_2 was bubbled through the solution to remove dissolved oxygen. The mixed solution was further magnetically stirred for 0.5h and the colour gradually from colourless to dark brown. The reaction solution was added into a Teflon-lined autoclave of 80mL capacity. The autoclave was heated and maintained at 160ºC for 18h. After being cooled to room temperature, the solid-state products was collected by high speed centrifuging at 10,000rpm and washed several times with de-ionized water and ethanol, then dried in a vacuum for 36h.

2.2 Characterization of Ag-doped ZnS nanocrystals

Powder X-ray diffraction (XRD) patterns were recorded on a Bruker D8 Advance X-ray powder diffractometer with graphite monochromatized Cu$K\alpha$ radiation (λ=0.15406nm). A scanning rate of 0.05deg•s^{-1} was applied to record the XRD pattern in the 2θ range of 20~70º. TEM and HRTEM measurements were carried out on a JEOL JEL-2010 transmission electron microscope with acceleration voltage of 100kV. A Shimadzu UV-2550 spectrophotometer was used to determine optical absorbance; samples were placed in quartz cuvettes (1cm path length). The photoluminescence (PL) spectra were performed at room temperature on a Hitachi F-7000 FL spectrophotometer with a 450 W xenon lamp as excitation source. All the optical measurements were performed at room temperature under ambient conditions.

3. Results and discussion
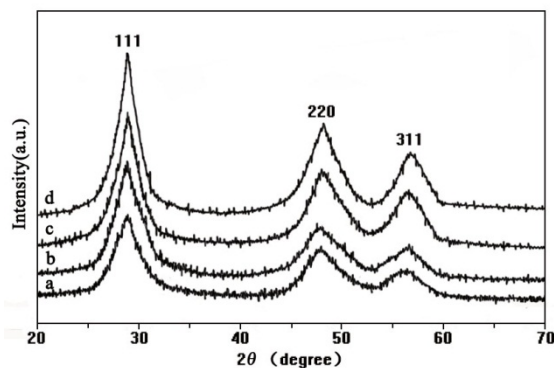
Fig. 1 XRD patterns of undoped ZnS (a) and Ag-doped ZnS nanocrystals (b: 0.5%; c: 1%; d: 2%)
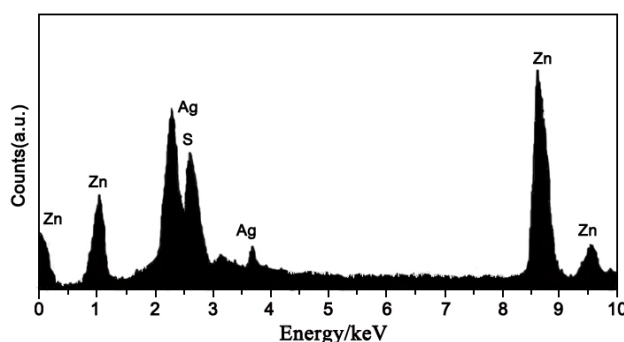
Fig. 2 EDX spectrum of as prepared Ag-doped ZnS nanocrystals.

Fig. 1 shows the XRD patterns of undoped ZnS and Ag-doped ZnS nanocrystals (molar ratio of Ag: Zn=0.5%, 1%, 2%) prepared in propanetriol solution by hydrothermal method. XRD pattern of samples exhibit peaks centred at 27.62º, 47.53º and 57.47º, which correspond to cubic phase structure of ZnS with three preferred orientations along with {111}, {220} and {311} planes. The peaks are well matched with standard PDF card for cubic ZnS (JCPDS NO. 05-0566). It is clear that the peaks are relatively broad, indicating that the nanoparticles have the small size. The nanocrystalline size is estimated according to the Debey-Scherrer equation:

$$D = \frac{k\lambda}{\beta \cos\theta} \tag{1}$$

where D is the mean grain size, k the constant (shape factor, approximately 0.9), λ the X-ray wavelength (0.15406nm for Cu$K\alpha$), β the full width at half maximum (FWHM) of the diffraction peak and θ the Bragg diffraction angle. The average size calculated for samples are 6.47nm, 6.79nm, 7.41nm and 7.96nm, while the corresponding molar ratio of Ag: Zn is 0, 0.5%, 1% and 2%. It can be seen that average size of nanocrystals increases as the doping percentage Ag ions is increased. The increase in particle size is also clear from the decrease in the FWHM of the XRD peaks. The energy dispersive X-ray (EDX) spectroscopy analysis showed that the nanocrystals contain Zn, Ag, and S, as illustrated in Fig. 2.
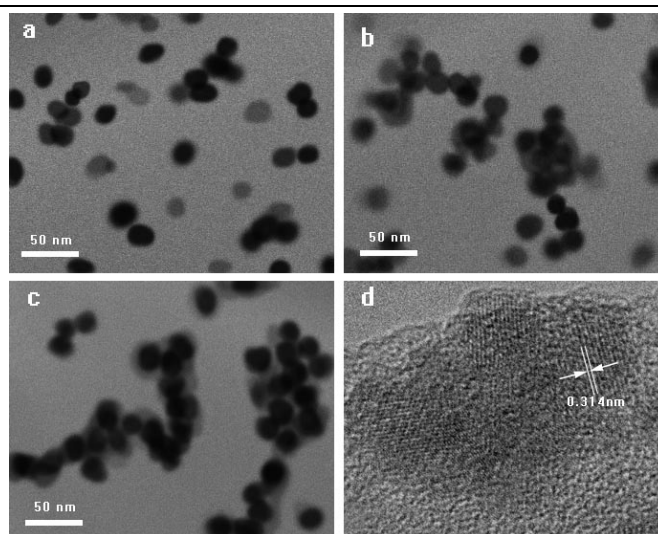
Fig. 3 TEM images of (a) undoped ZnS; (b) 1% Ag doped ZnS nanoparticles; (c) 2% Ag doped ZnS nanoparticles; (d) HRTEM image of 2% Ag doped ZnS nanoparticles
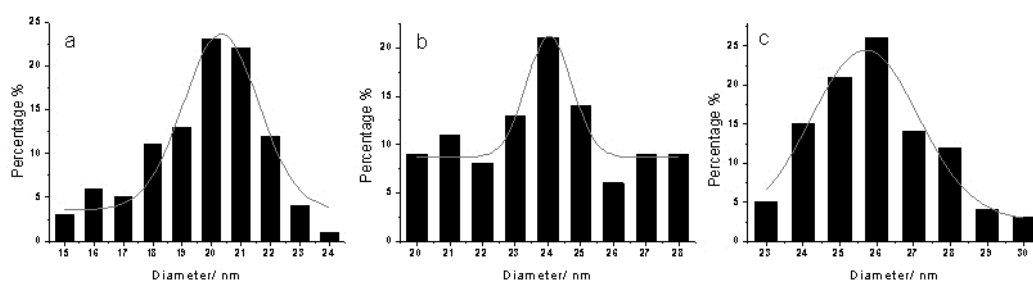
Fig. 4 Size distribution of (a) undoped ZnS; (b) 1% Ag doped ZnS nanoparticles;
(c) 2% Ag doped ZnS nanoparticles.

Fig. 3 shows the TEM and HRTEM images of undoped ZnS and Ag-doped ZnS nanocrystals from the typical experiments. From the TEM figures, these nanoparticles are approximately spherical in shape and obviously well dispersed. Fig. 4 shows the size distribution of undoped and Ag-doped ZnS nanocrystals, the average diameter of samples are 20.32±0.1497nm (undoped ZnS), 24.04±0.1333nm (Ag: Zn=1%), 25.70±0.1221nm (Ag: Zn=2%). It is becoming clear that the larger nanoparticles are associated with greater amounts of Ag dopant, which is in good agreement with the results of XRD characterization. The size of nanoparticles estimated from the TEM pictures is much larger than that of XRD results, which suggests that the obtained products are polycrystalline particles and also confirmed by HRTEM as shown Fig. 4d. The HRTEM image exhibits lattice fringes with d spacing of 0.314nm, indicating the formation of the cubic structure.
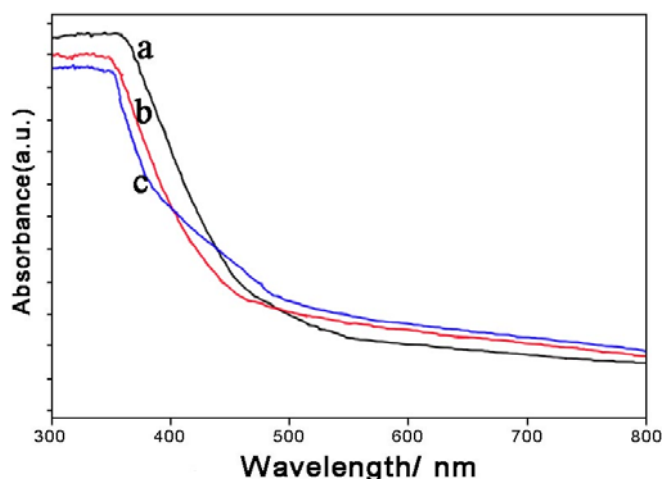
Fig. 5 UV-vis spectra of (a) undoped ZnS; (b) 1% Ag doped ZnS nanoparticles;
(c) 2% Ag doped ZnS nanoparticles.

The optical band gap of semiconductor nanocrystals increases with decreasing particle size due to quantum confinement effects. Fig. 5 shows the UV-vis absorption spectra of undoped and Ag-doped ZnS nanocrystals. The UV-vis spectra show a broad absorption peak without maximum appears in the range of 300~550nm. These optical spectra can be used to calculate the band gap from equation:

$$\alpha\,(h\nu) \sim (h\nu\text{-}E_g)^n \tag{2}$$

where α is absorption coefficient, h is Planck's constant and E_g is the optical band gap. The band gaps calculated for samples are 4.03ev, 3.89ev and 3.84ev, while the molar ratio of Ag: Zn are 0, 1% and 2%, respectively, which are higher than that of bulk ZnS (3.66ev) due to quantum size effect. The red shift in the absorption spectra edge is also found with increasing the content of Ag ions in the ZnS nanocrystals. This results obtained from the UV-vis spectra are consistent with the XRD results.
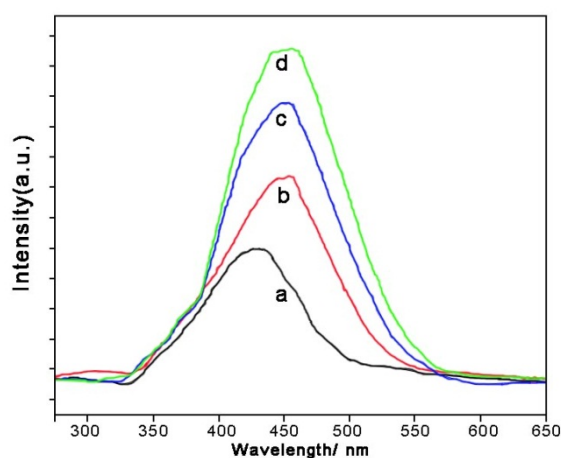
Fig. 6 PL spectra of (a) undoped ZnS; (b) 0.5% Ag doped ZnS nanoparticles; (c) 1% Ag doped ZnS
nanoparticles; (d) 2% Ag doped ZnS nanoparticles.

Room temperature photoluminescence (PL) spectra of ZnS nanocrystals with different amount of Ag ions (0, 0.5%, 1% and 2%) are shown in Fig. 6. The measurements were performed at an excitation wavelength of 350nm. The undoped ZnS nanocrystals exhibit an asymmetric emission feature at about 440nm. When ZnS was doped with silver, the PL emission peak shows at about 460nm which presents a red shift compared to the undoped ZnS nanocrystals. As the concentration of doped Ag ions increased from 0.5% to 2%, the PL peak intensity of the doped ZnS nanocrystals also increased significantly. It is well established that in semiconductor nanocrystals the emission occurs by the recombination of electrons and holes, which are the photo excited carriers, via various paths [15]. The PL spectra of ZnS nanocrystals are observed to be asymmetric and occurred at a lower energy value than that corresponding to the excitonic band. So it can be attributed to the recombination of the charge carrier trapped in the surface states. In our case, the emission can be assigned to the presence of sulphur vacancies. The increase of particle size with increase of Ag ions concentration results in the decrease of nanocrystals band gap energy, which may contribute to the red-shift of the PL emission peak. When Ag ions were incorporated into ZnS lattice, a great number of Ag ions would be present in the form of Ag_2S phase. Sulphur vacancies may be formed in the attachment region between the Ag_2S and ZnS phase. On the other hand, the Ag ions incorporated into ZnS lattice as an acceptor defect (Ag centres) also result in the enhancement of PL intensity of nanocrystals.

4. Conclusion

In conclusion, we reported the optical properties of Ag-doped ZnS nanocrystals prepared by hydrothermal method. XRD, TEM and UV-vis characterization show the increase in particle size with increasing doping concentration. The incorporation of silver in ZnS nanoparticles results in a different PL emission peak, which was enhanced significantly comparing with the undoped one. Due to good optical properties, the Ag-doped ZnS nanocrystals are expected to open up many opportunities for further fundamental studies and nanoscale optical applications.

References

[1] O. S. Oluwafemi, N. Revaprasadu, O. O. Adeyemi, Mater. Lett., **64**, 1513 (2010).
[2] H. Qu, L. Cao, G. Su, W. Liu, Y. Sun, B. Dong, J. Appl. Phys., **106**, 93506 (2009).
[3] C. S. Pathak, M. K. Mandal, Chalcogenide Lett., **8**, 147 (2011).
[4] G. Murugadoss, B. Rajamannan, U. Madhusudhanan, Chalcogenide Lett., **6**, 197 (2009).
[5] A. Chatterjee, A. Priyam, S. C. Bhattacharya, A. Saha, Colloid Surf. A, **297,** 258 (2007).
[6] C. Bi, L. Pan, Z. Guo, Y. Zhao, M. Huang, X. Ju, J. Q. Xiao, Mater. Lett., **64**, 1681 (2010).
[7] Z. Quan, Z. Wang, P. Yang, J. Lin, J. Fang, Inorg. Chem., **46**, 1354 (2007).
[8] M. L. Breen, A. D. Dinsmore, R. H. Pink, S. B. Qadri, B. R. Ratna, Langmuir, **17**, 903 (2001).
[9] W. Jian, J. Zhuang, D. Zhang, J. Dai, W. Yang, Y. Bai, Mater. Chem. Phys., **99**, 494 (2006).
[10] B. Dong, L. Cao, G. Su, W. Liu, H. Qu, H. Zhai, J. Alloy. Compd., **492**, 363 (2010).
[11] J. F. Suyver, S. F. Wuister, J. J. Kelly, A. Meijerink, Nano. Lett., **1**, 429 (2001).
[12] C. Mu, P. Liu, G. Zhu, X. Bian, J. Zhou, Y. He, Chinese J. Inorg. Chem., **23**, 844 (2007).
[13] J. Ge, J. Wang, H. Zhang, X. Wang, Q. Peng, Y. Li, Adv. Funct. Mater. **15**, 303 (2005).
[14] S. Sahai, M. Husain, V. Shanker, N. Singh, D. Haranath, J. Colloid Interf. Sci., **357**, 379 (2011).
[15] A. Murugadoss, A. Chattopadhyay, Bull. Mater. Sci., **31**, 533 (2008).
[16] H. Yang, C. Huang, X. Su, A. Tang, J. Alloy. Compd., **402**, 274 (2005).
[17] B. Geng, J. Ma, F. Zhan, Mater. Chem. Phys., **113**, 534 (2009).
[18] F. Huang, Y. Peng, C. Lin, Chem. Res. Chinese U., **22**, 675 (2006).
[19] H. Wang, H. Li, Chalcogenide Lett., **8**, 309 (2011).